DOI: 10.1002/cctc.201000213

The Effect of Organic Impurities Originating from the Incomplete Combustion of Organic Templates on the Methanol-to-Olefins Reaction over SAPO-46

Weili Dai, Wenbo Kong, Landong Li,* Guangjun Wu, Naijia Guan, and Niu Li*[a]

As an oil-free process to obtain olefins, the conversion of methanol-to-olefins (MTO) on microporous zeolite catalysts has attracted significant attention, since it was made known in 1977.[1–4] Subsequently, the mechanism of methanol conversion has been regarded as an intellectual challenge in heterogeneous catalysis. The MTO reaction is generally accepted to occur by a hydrocarbon pool mechanism, described as a catalytic scaffold composed of larger organic molecules adsorbed in the zeolites, to which methanol/dimethyl ether is added and from which alkenes and water are formed in a closed cycle.[6–9] A key issue in the hydrocarbon pool mechanism is the origin and specific constitution of the hydrocarbon pool. To obtain further information on this issue, extra organic species have been introduced to the MTO reaction system or MTO catalysts. For example, toluene has been employed as a cocatalyst for MTO reactions over ZSM-5, dealuminated mordenite, and beta zeolite.[10] Tetramethylphosphonium cations have been synthesized in the cages of H-SAPO-34 (like a ship in a bottle) and calcined to form methylnaphthalenes, as an active MTO catalyst.[11–13] The effect of the amount of coke already present in SAPO-34 on the selectivity of olefins has been studied.[14] The intrinsic organic contamination of calcined solid acids has already drawn great attention; for example Haw and co-workers described a very low, but detectable, amount of aromatic formation in SAPO-34 after calcination in static air at 600 °C for several hours. The organic impurities from the incomplete combustion of organic templates in the zeolite catalyst may be regarded as the primordial hydrocarbon pool to realize the MTO process.[15] The catalysts used for these processes are solid acids with strong Brönsted-acid sites (ZSM-5 or SAPO-34) and the secondary reactions quickly take place over these acids in the MTO process, leading to the formation of aromatics or cyclic organics as the new hydrocarbon pool. As a result, it is difficult to identify whether the incipient olefins are produced from the methanol reaction with the residual organic species or the newly formed hydrocarbon pool in the catalysts.

Therefore, a solid acid with a weaker acid strength and higher diffusivity may effectively prevent the secondary reactions and favor the understanding of the function of organic impurities in these catalysts. Herein we discuss how SAPO-46 samples calcined at different temperatures are investigated as catalysts for the MTO process. Special emphasis is placed on the effect of the organic species occluded in the cages due to the incomplete combustion of organic templates.

SAPO-46 (Figure 1) possesses a three-dimensional structure and supercage dimensions of approximately 1.30×0.98 nm, which are interconnected by a 12-membered ring (ca. 0.70 nm)

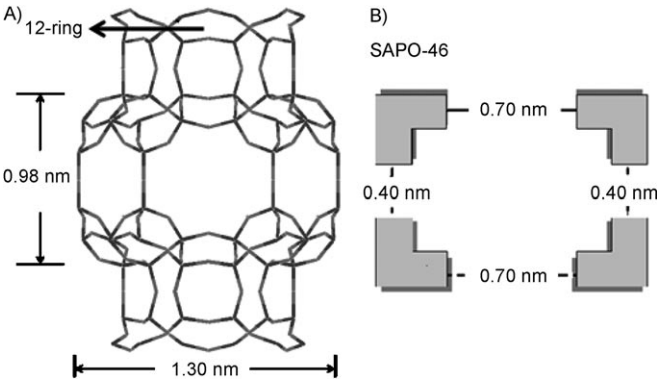

Figure 1. A) the cage and pore structure of SAPO-46; B) the cage structure in the framework.

and 8-membered ring windows (ca. 0.40 nm). The powder XRD patterns of SAPO-46 zeolites calcined at different temperatures (**a**: 350 °C; **b**: 400 °C; **c**: 450 °C; **d**: 500 °C) are shown in Figure S1 (see the Supporting Information). The intensity of the main diffraction peaks, which correspond to the structure of SAPO-46, gradually decreases with increasing calcination temperature. However, the structure of SAPO-46 is preserved for all samples.

The acidic properties of the samples employed in this study are evaluated by means of the temperature-programmed desorption of ammonia (NH_3-TPD; Figure 2 A). A low-temperature ammonia desorption peak at around 200 °C, attributed to weak acid sites, and a medium-temperature ammonia desorption peak at 300 °C, attributed to moderate acid sites, are observed for samples **b**–**d**. The intensities of these two peaks are quite similar, indicating a similar amount of acid sites in samples **b**–**d**. The low-temperature ammonia desorption peak at around 200 °C is much more intense for sample **a** than for the other samples, which may be a result of the mutual adsorption between organic impurities retained in the cages of sample **a** and ammonia. Nevertheless, no strong-acid sites were detected for SAPO-46 samples calcined at different temperatures.

[a] *W. Dai, W. Kong, Prof. L. Li, Dr. G. Wu, Prof. N. Guan, Prof. N. Li*
Key Laboratory of Advanced Energy Materials Chemistry (MOE)
College of Chemistry, Nankai University, Tianjin 300071 (PR China)
Tel./Fax: (+86) 22-23500341
E-mail: lild@nankai.edu.cn
liniu@nankai.edu.cn

Supporting information for this article is available on the WWW under http://dx.doi.org/10.1002/cctc.201000213.

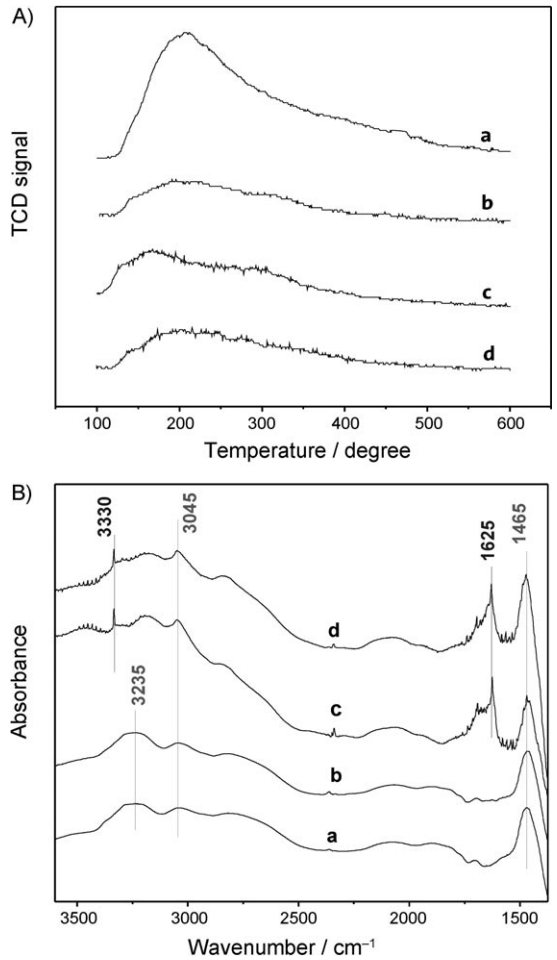

Figure 2. A) The NH_3-TPD profiles for SAPO-46 samples **a**–**d**; B) The FTIR spectra of NH_3 adsorption for SAPO-46 samples **a**–**d**.

The FTIR spectra of NH_3 adsorption were employed to obtain more information on the acidity of SAPO-46 (Figure 2B). For all of the SAPO-46 samples, NH_3 adsorbs on the Brønsted-acid sites in the form of ammonium ions, which are attributed to the peaks at $\tilde{\nu}=1465$ and 3045 cm^{-1}.[16] For samples **c** and **d**, NH_3 also adsorbs on the Lewis-acid center in the form of ammonia molecules, which are attributed to the peaks at $\tilde{\nu}=$ 1625 and 3330 cm^{-1}.[17] In contrast, no ammonia molecules on the Lewis acid center are detected for samples **a** and **b**, rather there is a broad peak centered at $\tilde{\nu}=3235$ cm^{-1}. Based on these results, it is concluded that similar Brønsted-acid sites exist in SAPO-46 calcined at different temperatures. For SAPO-46 calcined at higher temperatures, the Lewis-acid centers are exposed and are available for the adsorption of ammonia molecules. For SAPO-46 calcined at lower temperatures, the organic impurities retained in the cages may block the Lewis acid centers and form complexes with the ammonia molecules.[18]

The MTO reaction over the SAPO-46 catalyst was performed in a fixed-bed flow microreactor under atmospheric pressure at 450 °C. Samples **a** and **b** exhibit good activity for the MTO reaction in the initial 5 min. Typically, 100% methanol conversion with 35.3 and 41.3% selectivity to lower olefins ($C_{2=}$ and $C_{3=}$) is obtained for **a** and **b**, respectively. In addition to the lower alkane and olefins, some branched high-carbon hydrocarbons ($C_{>5}$) and aromatics (toluene and xylene) are present in the products of the MTO reaction over samples **a** and **b** (Figure 3A). These byproducts may be attributed to the unique shape selectivity induced by 12-ring pores. For samples **c** and **d**, the initial methanol conversion is below 80% and the dominant product is dimethyl ether (DME) with trace lower olefins (<1%). If the reaction proceeds over 90 min, DME becomes the dominant product over all samples (Figure 3B), indicating the rapid deactivation of samples **a** and **b**. According to the hydrocarbon pool mechanism, olefins can only be obtained from hybrid sites composed of acid sites and large organic intermediates that contain cyclic organics or aromatics. For SAPO-46 calcined at different temperatures, similar acid sites are present in samples **b**–**d** (Figure 2), therefore, their distinct behavior in the MTO reaction should be attributed to the different constitutions of the residual organic species from the incomplete combustion of the organic templates.

The exact constitution of the organic species originating from the incomplete combustion of organic template in the SAPO-46 samples was analyzed by means of GC-MS. 2-Benzenedicarboxylic acid dibutyl ester (DBP), hexadecane, and 2,6,10,14-tetramethyl-pentadecane were detected in all samples (Figure 4A). As samples **c** and **d** do not exhibit clear activity for the MTO reaction, these species (DBP and the higher alkanes) should not be the active organic species for the production of olefins. Besides DBP and the higher alkanes, toluene and benzyl alcohol were detected in samples **a** and **b**. Considering the noticeable olefin production over both samples **a** and **b**, we propose that toluene and/or benzyl alcohol are the so-called active organic species in the MTO process. To obtain further insight into the role of the residual organic species, toluene and benzyl alcohol were used as tracers (1 mol%) in the reactant during the MTO process over sample **d**. When benzyl alcohol was used as the tracer in the reactant, no MTO reaction was observed. When toluene was used as the tracer, the MTO reaction took place over sample **d** and olefins were detected in the products (see the Supporting Information, Figure S2). Clearly, trace toluene plays a key role in realizing the MTO process. Based on the above results, we can confirm that toluene is the primordial hydrocarbon pool, or a precursor for the formation of the primordial hydrocarbon pool, that induces the initial MTO reaction. To obtain information on the transformation of the residual organic species in SAPO-46 during the MTO reaction, the occluded organic species in samples **a** (with MTO activity) and **d** (without MTO activity) after reaction for 6 h are carefully analyzed. As seen in Figure 4B, polymethylbenzenes and alkylnaphthalenes with 1–2 fused benzene rings are observed in sample **a** after the reaction, whereas, the residual toluene could no longer be observed. We propose that, under the MTO reaction conditions, the initial toluene is transformed to polymethylbenzenes and alkylnaphthalenes, from which olefins can be produced through "paring" or "side-chain" routes (Scheme 1).[9,19–22] After the MTO reaction over sample **d**, traces of xylene and trimethylbenzene were observed, indicating that these species can be formed in the

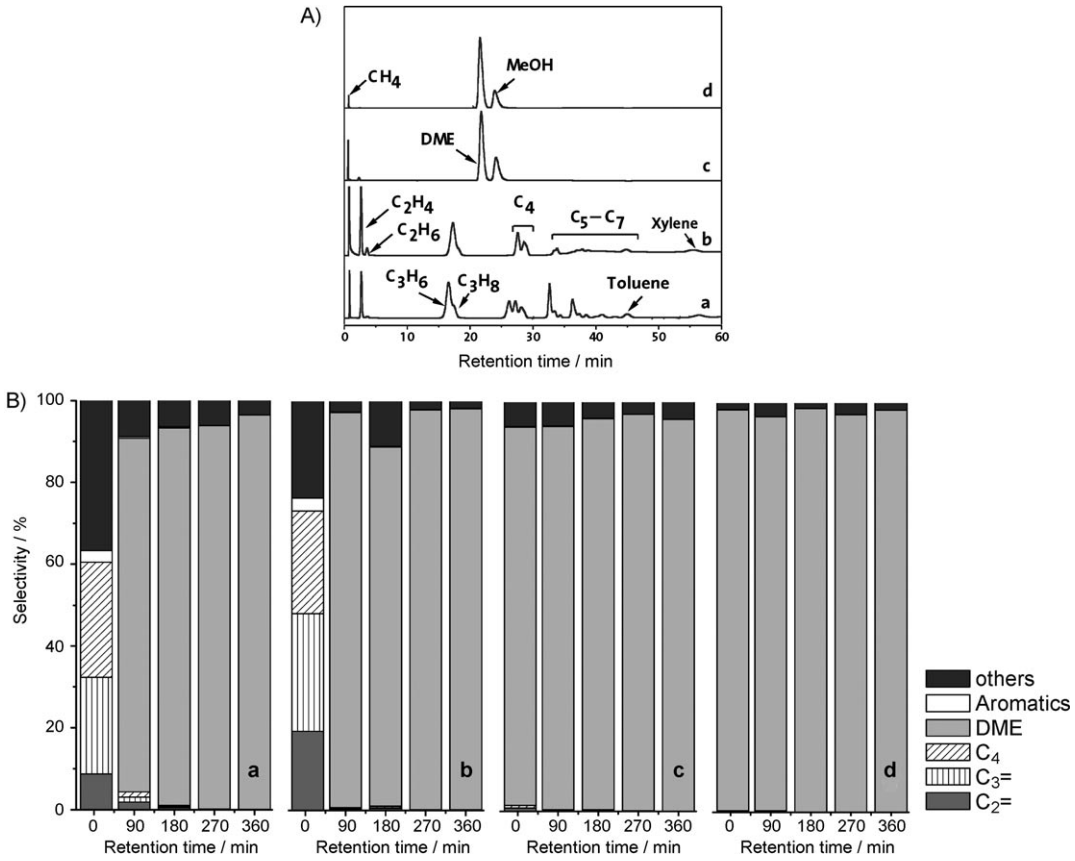

Figure 3. A) The GC profiles of methanol pulsed onto samples **a**–**d** at 450 °C for the initial 5 min; B) Time-dependent product selectivity in MTO reaction over samples **a**–**d**.

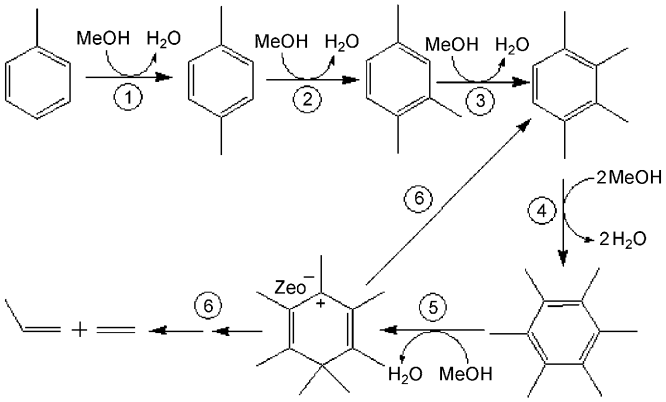

Scheme 1. Initiating step for the formation of olefins from methylbenzene.

presence of weak-acid sites in SAPO-46. However, the amount of these species is quite low and is not sufficient for the production of olefins. Notably, when toluene was used as the tracer in the reactant, a considerable amount of polymethylbenzenes and DBP were detected in sample **d** after the reaction (see the Supporting Information, Figure S3). The results further confirm that toluene can be transformed into polymethylbenzenes, a well-known hydrocarbon pool, during the reaction.

In conclusion, organic impurities that originate from the incomplete combustion of the organic template may play a decisive role in the MTO reaction over zeolite catalysts. For the zeolite SAPO-46, the organic impurities toluene, benzyl alcohol, DBP, and some higher alkanes are detected from samples calcined under certain conditions. Amongst these impurities, toluene may be the primordial hydrocarbon pool, or the precursor for the formation of the primordial hydrocarbon pool, that induces the initial MTO reaction. Under the MTO reaction conditions, residual toluene in SAPO-46 can be transformed to polymethylbenzenes and alkylnaphthalenes, that is, the well-known active hydrocarbon pool for the MTO process. The results reported herein not only benefit the further understanding of the hydrocarbon pool mechanism in the MTO process, but also aid the design of new MTO catalysts.

Experimental Section

SAPO-46 zeolite was synthesized by means of a one-step route with di-*n*-propylamine as the template, details of which can be found in our previous report.[23] The chemical composition of SAPO-46 employed in this study is Si/P/Al = 0.20:0.42:0.58. Most silicon atoms in SAPO-46 are located on the tetrahedral phosphorus sites of the $AlPO_4$ framework, as established by the respective ^{29}Si MAS NMR spectroscopy study. The as-prepared SAPO-46 was calcined in flowing air at different temperatures for 3 h, followed

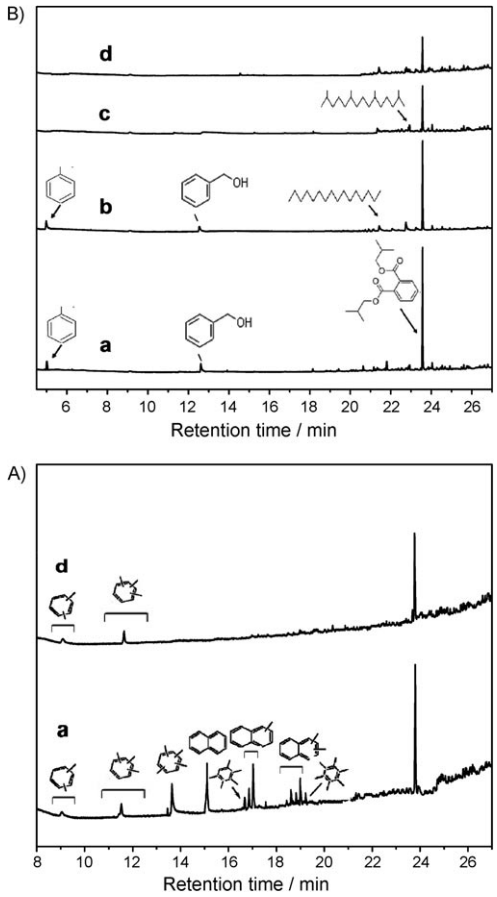

Figure 4. A) The GC-MS chromatograms of extracts from SAPO-46 calcined at different temperatures (samples **a**–**d**); B) Samples **a** and **d** after the MTO reaction at 450 °C for 6 h .

by calcination in flowing nitrogen at 450 °C for 1 h. Samples of SAPO-46 were calcined in flowing air at 350 °C, 400 °C, 450 °C and 500 °C, to produce samples **a**, **b**, **c**, and **d**, respectively.

The temperature-programmed desorption of ammonia (NH_3-TPD) was completed in a quartz U-shaped reactor and was monitored by using an online chemisorption analyzer (Quantachrome ChemBet 3000). A sample (ca. 0.1 g) was pretreated at 600 °C for 1 h in an He flow (30 mL min^{-1}), cooled to 100 °C, and saturated with 5% NH_3/Ar. After that, the sample was purged with He for enough time to eliminate the physically absorbed ammonia. NH_3-TPD was then completed in the range of 100–600 °C at a heating rate of 10 °C min^{-1}.

The NH_3 adsorption was measured by means of FTIR spectroscopy by using a Bruker Tensor 27 spectrometer with a MCT detector at a resolution of 4 cm^{-1}. A self-supporting pellet made of the sample was placed in the IR flow cell and the reference spectrum was taken at room temperature. After NH_3 dosing at room temperature for 30 min, the FTIR spectra of the NH_3 saturated adsorption samples were recorded.

In each MTO experiment, the catalyst (ca. 0.4 g) was loaded into a stainless steel tube (5 mm i.d.) and pretreated in nitrogen flow (20 mL min^{-1}) at 450 °C for 1 h. Methanol was then pumped in at 0.5 mL h^{-1} (WHSV = 1 h). The products were analyzed online by using a gas chromatograph equipped with a flame ionization detector and a packed-column Porapak Q for the separation of C_1–C_4 hydrocarbons and other higher hydrocarbons.

For GC-MS analysis, a catalyst sample (ca. 0.3 g) was taken after the reaction and carefully dissolved in 1 M HCl solution (20 mL). The solution was treated with CH_2Cl_2 (10 mL), to extract the organic materials. A sample of CH_2Cl_2 (ca. 1.0 μL) organic extract was analyzed by using GC-MS (Agilent 7890A/5975 MSD) with a DB-5 MS column (30 m, 0.25 mm i.d., stationary phase thickness 0.25 μm). The following temperature program was employed: Isothermal at 40 °C for 6 min and then heated to 280 °C at a ramping rate of 10 °C min^{-1}.

Acknowledgements

This work was financially supported by the National Basic Research Program of China (973 Program 2009CB623502).

Keywords: heterogeneous catalysis · hydrocarbon pool mechanism · impurities · olefins · zeolites

[1] C. D. Chang, A. J. Silvestri, *J. Catal.* **1977**, *47*, 249 – 259.
[2] J. F. Haw, W. G. Song, D. M. Marcus, J. B. Nicholas, *Acc. Chem. Res.* **2003**, *36*, 317 – 326.
[3] B. Arstad, S. Kolboe, *J. Am. Chem. Soc.* **2001**, *123*, 8137 – 8138.
[4] W. Wang, M. Hunger, *Acc. Chem. Res.* **2008**, *41*, 895 – 904.
[5] M. Stöcker, *Microporous Mesoporous Mater.* **1999**, *29*, 3 – 48.
[6] I. M. Dahl, S. Kolboe, *J. Catal.* **1994**, *149*, 458 – 464.
[7] I. M. Dahl, S. Kolboe, *J. Catal.* **1996**, *161*, 304 – 309.
[8] P. W. Goguen, T. Xu, D. H. Barich, T. W. Skloss, W. G. Song, Z. Wang, J. B. Nicholas, J. F. Haw, *J. Am. Chem. Soc.* **1998**, *120*, 2650 – 2651.
[9] S. Svelle, F. Joensen, J. Nerlov, U. Olsbye, K-P. Lillerud, S. Kolboe, M. Bjørgen, *J. Am. Chem. Soc.* **2006**, *128*, 14770 – 14771.
[10] Ø. Mikkelsen, P. O. Rønning, S. Kolboe, *Microporous Mesoporous Mater.* **2000**, *40*, 95 – 113.
[11] W. G. Song, J. F. Haw, *Angew. Chem.* **2003**, *115*, 920 – 922; *Angew. Chem. Int. Ed.* **2003**, *42*, 892 – 893.
[12] W. G. Song, H. Fu, J. F. Haw, *J. Phys. Chem. B* **2001**, *105*, 12839 – 12843.
[13] M. Bjørgen, U. Olsbye, D. Petersen, S. Kolboe, *J. Catal.* **2004**, *221*, 1 – 10.
[14] Y. A. Wei, D. Z. Zhang, F. X. Chang, Q. H. Xia, B. L. Su, Z. M. Liu, *Chem. Commun.* **2009**, 5999 – 6001.
[15] W. G. Song, D. M. Marcus, H. Fu, J. O. Ehresmann, J. F. Haw, *J. Am. Chem. Soc.* **2002**, *124*, 3844 – 3845.
[16] A. Zecchina, L. Marchese, S. Bordiga, C. Paze, E. Gianotti, *J. Phys. Chem. B* **1997**, *101*, 10128 – 10135.
[17] G. V. A. Martins, G. Berlier, C. Bisio, S. Coluccia, H. O. Pastore, L. Marchese, *J. Phys. Chem. C* **2008**, *112*, 7193 – 7200.
[18] K. Nakamoto, *Infrared and Raman spectra of inorganic and coordination compounds*, Wiley, New York, **1997**.
[19] D. M. McCann, D. Lesthaeghe, P. W. Kletnieks, D. R. Guenther, M. J. Hayman, V. V. Speybroeck, M. Waroquier, J. F. Haw, *Angew. Chem.* **2008**, *120*, 5257 – 5260; *Angew. Chem. Int. Ed.* **2008**, *47*, 5179 – 5182.
[20] D. M. Marcus, W. G. Song, S. M. Abubakar, E. Jani, A. Sassi, J. F. Haw, *Langmuir* **2004**, *20*, 5946 – 5951.
[21] D. Lesthaeghe, B. D. Sterck, V. Van Speybroeck, G. B. Marin, M. Waroquier, *Angew. Chem.* **2007**, *119*, 1333 – 1336; *Angew. Chem. Int. Ed.* **2007**, *46*, 1311 – 1314.
[22] B. Arstad, J. B. Nicholas, J. F. Haw, *J. Am. Chem. Soc.* **2004**, *126*, 2991 – 3001.
[23] W. B. Kong, W. L. Dai, N. Li, N. J. Guan, S. H. Xiang, *J. Mol. Catal. A: Chem.* **2009**, *308*, 127 – 133.

Received: June 21, 2010
Revised: July 23, 2010
Published online on October 12, 2010

